

# Laser Research Center for Molecular Science

## VIII-B Developments of Advanced Lasers for Chemical Reaction Controls and ZEKE Photoelectron Spectroscopy

### VIII-B-1 Developments of Liquid Crystal Spatial Light Modulator

SATO, Shin-ichiro; WATANABE, Kazuo

The chemical reaction controls with laser lights are one of the most important subjects of chemistry. The coherence of laser lights has not been considered seriously in the old fashion of the laser controls of chemical reactions. Recent theoretical studies have shown that the more sophisticated controls of chemical reactions. As a first step, we are trying to maximize efficiency of the quantum transition with a chirped ultra short pulsed laser. This technique is based on an adiabatic passage theory of quantum transitions. We are developing a photo waveform shaper of ultra short laser pulses to make an arbitrary shaped pulse, including chirped ones. The spectral components of the incident pulse are spatially dispersed with a grating, modulated or retarded with a liquid crystal array on the Fourier plane and recombined with another grating.

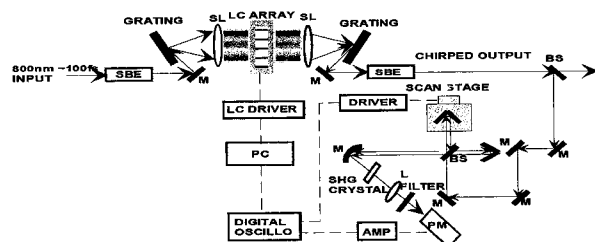


**Figure 1.** Schematic diagram of liquid crystal spatial light modulator.

### VIII-B-2 ZEKE Electron Spectroscopy of Azulene and Azulene-Argon

TANAKA, Daisaku; SATO, Shin-ichiro; KIMURA, Katsumi

Mass-selected ion-current spectra and zero-kinetic-energy (ZEKE) electron spectra were obtained for azulene and its van der Waals (vdW) complex with Ar in supersonic jets by two-photon ( $1 + 1'$ ) resonant ionization through the second singlet electronic excited state ( $S_2$ ). Ab initio calculations were also carried out to study the optimized geometry and vibrational modes for azulene in the neutral and cation ground states ( $S_0$  and  $D_0$ ). Lennard Jones (LJ) potential energy calculations including "charge-charge-induced-dipole interactions" were also made for azulene-Ar. The main results may be summarized as follows. (1) The adiabatic ionization energies have been determined as  $I_a$  (azulene) =  $59781 \pm 5 \text{ cm}^{-1}$  and  $I_a$  (azulene-Ar) =  $59708 \pm 5 \text{ cm}^{-1}$ . The difference in  $I_a$  is  $73 \text{ cm}^{-1}$ . (2) Several vibrational frequencies of (azulene)<sup>+</sup> have been observed and identified on the basis of ab initio theoretical calculations. (3)

vibrational progression with a spacing of  $9\text{--}10 \text{ cm}^{-1}$  in the ZEKE spectra of azulene-Ar has been assigned experimentally and theoretically to the vdW bending vibration  $b_x^{+1}$  along the long axis of azulene. (4) From the calculated LJ potential energy minima, it has been found that Ar is shifted by  $0.10 \text{ \AA}$  along the long axis of azulene from the position in the neutral ground state. (5) The observed vdW vibrational progressions have been reproduced by Franck-Condon calculations, suggesting that Ar is shifted by  $2^\circ$  for (azulene-Ar)<sup>+</sup> with respect to its neutral  $S_2$  state.

## VIII-C Developments and Researches of New Laser Materials

Although development of lasers is remarkable, there are no lasers which lase in ultraviolet and far infrared regions. However, it is expected that these kinds of lasers break out a great revolution in not only the molecular science but also in the industrial world.

In this project we research characters of new materials for ultraviolet and far infrared lasers, and develop new lasers by using these laser materials.

### VIII-C-1 Intense THz Radiation from Femtosecond Laser Pulses Irradiated InAs in a Strong Magnetic Field

OHTAKE, Hideyuki; ONO, Shingo<sup>1</sup>; KAWAHATA, Eiji; LIU, Zhenlin; SARUKURA, Nobuhiko  
(<sup>1</sup>Sci. Univ. Tokyo)

Since the first observation of THz radiation from InAs surface irradiated with femtosecond laser pulses, considerable effort have been made to design an intense THz-radiation source and to understand the mechanism for generating THz radiation. However, the problem has not been solved. In this paper, we have investigated the intense THz radiation from InAs by applying a strong magnetic field up to 5 T. We compared several different geometries. Besides quadratic magnetic field dependence, we found saturation of the THz-radiation intensity around 3 T. Furthermore, the intensity decreased dramatically above 3 T. It represented that the most suitable magnetic field was 3 T to design an intense THz-radiation source. We also took spectra by a Polarizing Michelson interferometer. The spectral shapes for the different magnetic field directions were significantly different. The center frequency of these spectra shifted to lower frequency with increasing magnetic field. Through these experiments, we found the best configuration and the most suitable magnetic field to obtain an intense THz radiation for various applications such as imaging, sensing, and spectroscopy. This configuration dependence of the spectral shape and the center frequency is attributed to be the initial carrier acceleration processes modulated by a strong magnetic field.

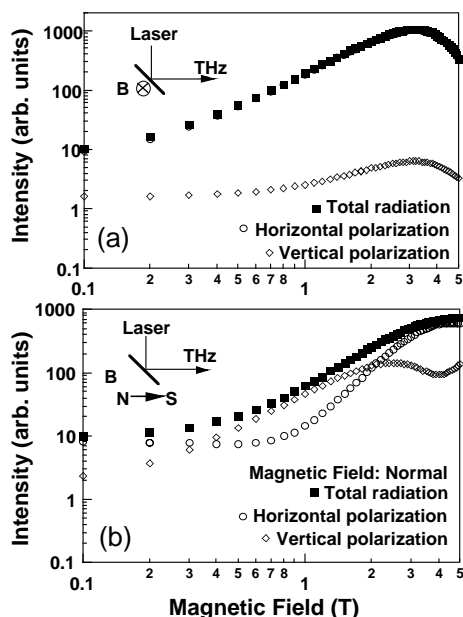


**Figure 1.** Magnetic field dependence of THz-radiation intensity. Inset indicates the experimental geometry. Closed squares, open circle and diamonds show total radiation, horizontal and vertical polarization, respectively. (a) The saturation of THz radiation intensity is clearly observed. (b) The saturation is not observed.

### VIII-C-2 High-Repetition-Rate, High-Average-Power Mode-Locked Ti:sapphire Laser with an Intracavity cw-Amplification Scheme

LIU, Zhenlin; ONO, Shingo<sup>1</sup>; KOZEKI, Toshimasa; OHTAKE, Hideyuki; SARUKURA, Nobuhiko  
(<sup>1</sup>Sci. Univ. Tokyo)

We have demonstrated a high-average-power, mode-locked Ti:sapphire laser with an intracavity cw-amplification scheme. The laser generated 150-fs pulses with 3.4-W average power at a repetition rate of 79 MHz. This simple amplification scheme can be applied for the power scaling of other lasers.

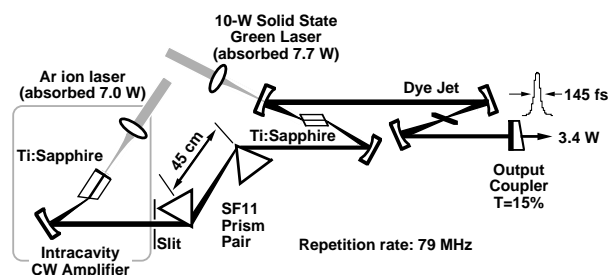


**Figure 1.** Configuration of high-repetition-rate high-average-power (3.4 W) femtosecond Ti:sapphire laser with an intracavity cw amplifier. The half-cut Brewster Ti:sapphire crystal composed the intracavity cw amplifier.

### VIII-C-3 Compact THz-radiation Source Consisting of a Bulk Semiconductor, a Mode-Locked Fiber Laser, and a 2-T Permanent Magnet

ONO, Shingo<sup>1</sup>; TSUKAMOTO, Takeyo<sup>1</sup>; KAWAHATA, Eiji; LIU, Zhenlin; OHTAKE, Hideyuki; SARUKURA, Nobuhiko; NISHIZAWA, Seizi<sup>2</sup>; NAKANISHI, Akio<sup>3</sup>; YOSHIDA, Makoto<sup>4</sup>  
(<sup>1</sup>Sci. Univ. Tokyo; <sup>2</sup>JASCO Co.; <sup>3</sup>Sumitomo Special Metals co., Ltd.; <sup>4</sup>IMRA AMERICA, INC. JLO)

Various THz-radiation sources have been intensively studied including photo conductive switches irradiated with ultrashort optical pulses. An intense, compact, and simple light source is required for applications in sensing or imaging. We have demonstrated the strong enhancement of THz-radiation power with a magnetic

field by using an InAs semiconductor. In this paper, we report on a compact THz-radiation source consisting of a fiber femtosecond laser and a newly designed 2-T permanent magnet shown in Figure 1. A mode-locked frequency doubled Er-doped fiber laser delivered 170-fsec pulses at 780 nm with a 48.5-MHz repetition rate (IMRA model FA7850/10SA) with 30-mW average power and 4.1-kW peak power. The mode-locked fiber laser is a completely turn-key system. It is much smaller than a mode-locked Ti:sapphire laser that requires daily alignment. The used semiconductor sample was undoped bulk InAs with a (100) surface. The 2-T permanent magnet unit consisted of 8 Nd-Fe-B magnet pieces. The remanence magnetic field of the Nd-Fe-B material itself was 1.3 T (NEOMAX-44H). Owing to the new magnetic circuit design, the magnetic field in the center exceeded the remanence magnetic field of the material. The permanent magnet only weighs about 5 kg. The 2-T permanent magnet unit is smaller and much lighter than an electromagnet. At present the average power is estimated to sub-micro watt level. The spectra of the THz radiation were obtained by a Polarizing Michelson interferometer. Many water vapor absorption lines were clearly observed. Therefore, the THz-radiation source is already usable for spectroscopy. Such a simple and compact source will open up new application for THz-radiation.

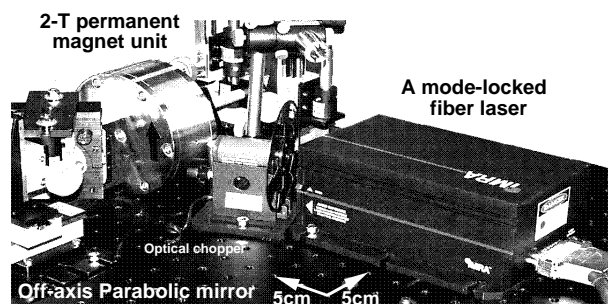


**Figure 1.** Photograph of a compact THz-radiation source with a bulk semiconductor, a fiber femtosecond laser, and a 2-T permanent magnet. Including the laser, the size is less than 40 × 30 × 15 cm.

#### VIII-C-4 Spectrum Control of THz Radiation from InAs in a Magnetic Field by Duration and Frequency Chirp of the Excitation Pulses

**KAWAHATA, Eiji; ONO, Shingo<sup>1</sup>; LIU, Zhenlin; OHTAKE, Hideyuki; SARUKURA, Nobuhiko**  
(<sup>1</sup>Sci. Univ. Tokyo)

The THz-radiation spectrum from InAs in a magnetic field irradiated with femtosecond pulses can be controlled by varying the excitation pulse width and chirp direction of the excitation pulse. A longer excitation pulse width produces lower frequency THz radiation. Also, positively chirped pulse excitation will generate higher power and higher frequency THz radiation, due to the corruption of the impulse response of the semiconductor in the longer pulse width region. The spectral shape of the radiation strongly depends on the chirp direction. This unexpected difference with the same excitation peak power and the same pulse duration

with different chirp direction is rather surprising. This difference of THz-radiation for the chirping of the excitation pulses might be attributed to the difference of the photo-carrier relaxation process in the conduction band with oppositely chirped-pulse excitation.

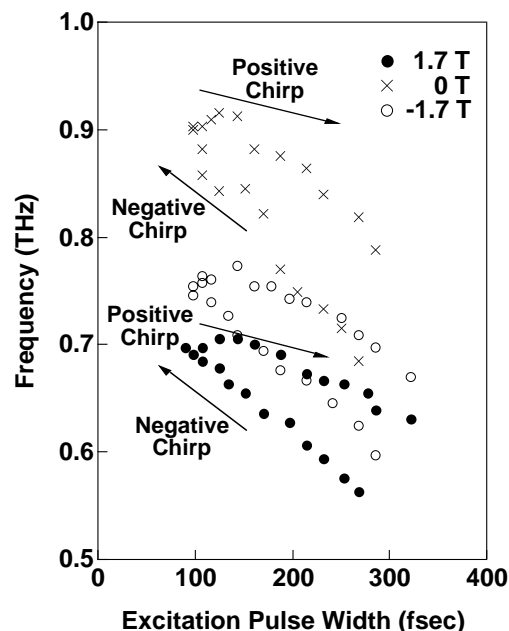


**Figure 1.** Center frequency spectrum dependence of THz radiation with different excitation chirp, pulse duration and magnetic field. Close circle, open circle and cross show 1.7 T, -1.7 T and 0 T, respectively.

#### VIII-C-5 LiCAF Crystal as a New Vacuum Ultraviolet Optical Material with Transmission down to 112 nm

**KOZEKI, Toshimasa; SAKAI, Masahiro; LIU, Zhenlin; OHTAKE, Hideyuki; SARUKURA, Nobuhiko; SEGAWA, Yusaburo<sup>1</sup>; OBA, Tomoru<sup>2</sup>; SHIMAMURA, Kiyoshi<sup>3</sup>; BALDOCHI, Sonia L.<sup>3</sup>; NAKANO, Kenji<sup>3</sup>; MUJILATU, Na<sup>3</sup>; FUKUDA, Tsuguo<sup>3</sup>**  
(<sup>1</sup>RIKEN; <sup>2</sup>Optron Inc.; <sup>3</sup>Tohoku Univ.)

LiCaAlF<sub>6</sub> (LiCAF) was found to be an ideal optical material for the vacuum ultraviolet region due to its superior transmission characteristic of down to 112 nm, its non hydroscopic nature, and its better mechanical properties compared with LiF.

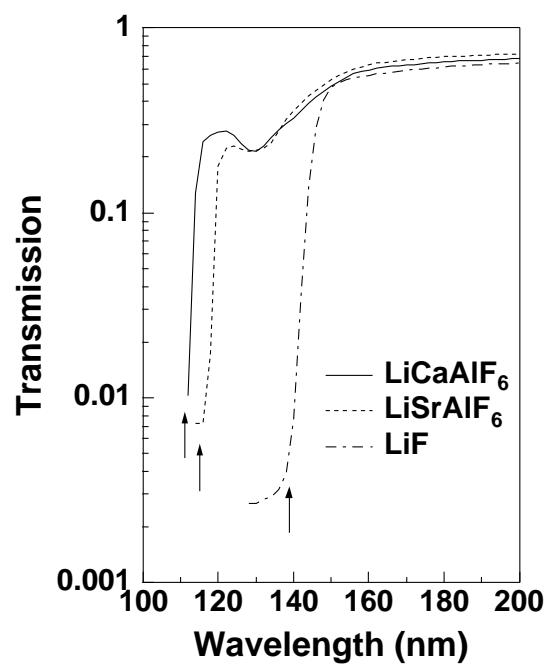


Figure 1. Transmission characteristics of LiCAF, LiSAF, LiF.

## VIII-D Development and Research of Advanced Tunable Solid State Lasers

Diode-pumped solid-state lasers can provide excellent spatial mode quality and narrow linewidths. The high spectral power brightness of these lasers has allowed high efficiency frequency extension by nonlinear frequency conversion. Moreover, the availability of new and improved nonlinear optical crystals makes these techniques more practical. Additionally, quasi phase matching (QPM) is a new technique instead of conventional birefringent phase matching for compensating phase velocity dispersion in frequency conversion. These kinds of advanced tunable solid-state light, so to speak Chroma Chip Lasers, will assist the research of molecular science.

In this projects we are developing Chroma Chip Lasers based on diode-pumped-microchip-solid-state lasers and advanced nonlinear frequency conversion technique.

### VIII-D-1 Frequency-Doubled Tunable Yb:YAG Microchip Laser for Holographic Volume Memories

SAIKAWA, Jiro; TAIRA, Takunori

Holographic volume memories have provoked a great deal of controversy.<sup>1)</sup> Angle and wavelength-multiplexed recordings have excellent potential for a large storage capacity.<sup>2,3)</sup> However, large cumbersome light sources prevent the research of holographic data storage systems. Lately, we developed diode-pumped single-frequency and tunable Yb:YAG microchip laser.<sup>4)</sup> In this work, we have demonstrated multiplex recording by using an intracavity frequency doubled Yb:YAG green laser.

The experimental configuration is shown in Figure 1. The frequency-doubled Yb:YAG laser consists of 400- $\mu\text{m}$  thickness YAG doped with 25 at.% Yb<sup>3+</sup> ion assembled on a sapphire substrate. Because the internal surface of the Yb:YAG microchip has partial reflectivity for laser wavelength, this microchip acts as a mode selection etalon. For tuning, a 1 mm thickness quartz plate was inserted into the laser cavity as a birefringent filter. A 2 mm KTP crystal was cut for type-II second-harmonic (SH) phase matching ( $\theta = 90^\circ$ ,  $\phi = 50^\circ$ ). In the frequency doubled Yb:YAG laser, tuning from 514.8 to 525.7 nm (10.9 nm, 12.4 THz) and maximum SH output power of 112 mW were obtained with single-axial-mode.

The recording medium was a 1% Fe-doped LiNbO<sub>3</sub> (Fe:LN) single crystal (3 × 3 × 5 mm). The *c*-axis of the crystal was parallel to the grating vector of the hologram. A reference beam *R* and a signal beam *S* irradiated opposite sides of the crystal, both at an angle  $\theta_0$  of 10°. A pattern mask with a 10 × 10 mm<sup>2</sup> character image, two lenses (diameter:  $d = 1\text{-inch}$ , focal length  $f = 75.5\text{-mm}$ ), the Fe:LN crystal, and a CCD camera made a Fourier-transform holographic system. We recorded and reconstructed two successive wavelength-multiplexed holograms by using light of two wavelengths that were 0.31 nm apart which corresponds to the FSR of 400- $\mu\text{m}$  Yb:YAG microchip.

#### References

- 1) J. F. Heanue *et al.*, *Science* **265**, 749 (1994).
- 2) S. Campbell and P. Yeh, *Appl. Opt.* **35**, 2380 (1996).
- 3) T. Kume *et al.*, *Jpn. J. Appl. Phys.* **35**, 448 (1996).
- 4) T. Taira *et al.*, *IEEE J. Sel. Top. Quantum Electron.* **3**, 100 (1997).

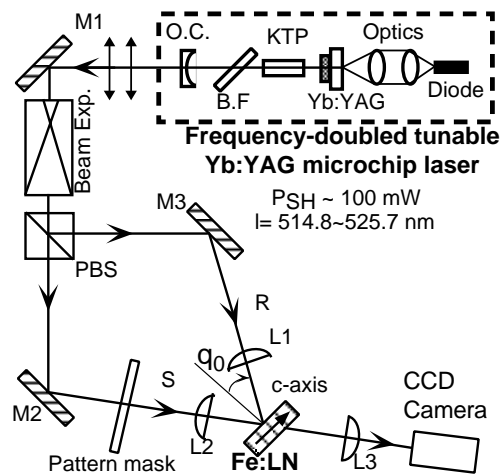


Figure 1. Holographic recording system by using intracavity frequency-doubled Yb:YAG microchip laser.

### VIII-D-2 Design Criteria for Optimization of Fiber-Coupled Diode Longitudinally-Pumped Laser Using Pump-beam $M^2$ Factor

PAVEL, Nicolaie<sup>1</sup>; KURIMURA, Sunao; TAIRA, Takunori

(<sup>1</sup>*Inst. Atm. Phys., Romania*)

For optimization of longitudinally-pumped solid-state lasers, a model which consider the pump-beam propagation described by its  $M^2$  factor is proposed. Analytical functions for the optimum focusing-position, the optimum pump spot-size, the minimum threshold pump power and the maximum overlap efficiency are given. A simple output to input power relation and previous formula provides a straightforward procedure to design the optimum laser resonator, the coupling-optics and to evaluate the laser output power.

A slope efficiency of 57% with a 53% optical-efficiency at maximum 8-W pump-power was obtained from a fiber-coupled longitudinally-pumped Nd:YAG medium. A very good agreement between experiments and theory was obtained.

#### References

- 1) R. A. Fields *et al.*, *Appl. Phys. Lett.* **51**, 1885 (1987).
- 2) T. Taira *et al.*, *Opt. Lett.* **16**, 1955 (1991).
- 3) M. D. Selker *et al.*, *CLEO CPD21*, (1996).
- 4) T. Taira *et al.*, *OSA TOPS* **19**, 430 (1998).

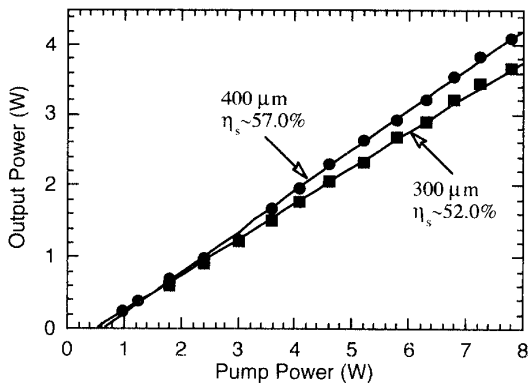


Figure 1. Output power as a function of pump-power.

### VIII-D-3 Highly Nd<sup>3+</sup>-Doped YAG Ceramic for Microchip Lasers

TAIRA, Takunori; KURIMURA, Sunao; SAIKAWA, Jiro; IKESUE, Akio<sup>1</sup>; YOSHIDA, Kunio<sup>2</sup>  
(<sup>1</sup>JFCC; <sup>2</sup>Osaka Inst. Tech.)

Nd:YVO<sub>4</sub> offers highly efficiency miniature or microchip lasers due to its high absorption and emission cross-sections.<sup>1-4</sup> However, its poor thermo-mechanical properties prevent high power laser operation. Much effort has gone into laser material research to find a high absorption coefficient laser medium with high thermal shock parameters. Lately, a high optical quality Nd:YAG laser material of polycrystalline ceramic has been reported.<sup>5</sup> In this paper, we have demonstrated a highly efficient oscillation in a Nd:YAG ceramic microchip laser.

The YAG ceramic allows highly neodymium-ion doping to overcome low absorption cross-section. The absorption coefficient of the single Nd:YAG crystal was 3.45 cm<sup>-1</sup> at 808 nm, while the 9.1 at.% Nd:YAG ceramic has about 10 times higher absorption. The absorption coefficient of the 4.8 at.% Nd:YAG ceramic was 11.7 cm<sup>-1</sup>. This result indicates that Nd:YAG ceramic has advantages in a microchip or miniature laser system as well as Nd:YVO<sub>4</sub>. The thermal conductivity of Nd:YAG ceramic decreases with Nd concentration and thermal conductivity of the 9.1 at.% doped YAG ceramic was 9.0 W/mK.

The 4.8 at.% Nd<sup>3+</sup> doped YAG ceramic was cut to a 847 μm thickness for microchip laser experiments. The plan-concave resonator configuration has an output mirror radius of 100-mm and a resonator length of 50-mm. The 808 nm pump beam was focused to a diameter of 100 μm in the medium. Figure 1 shows an output power of Nd:YAG ceramic laser as a function of input power. A performance of 0.9 at.% Nd:YAG single crystal also plotted in order to compare. As a result, the maximum output power of Nd:YAG ceramic laser was four times higher than conventional Nd:YAG single crystal laser because the YAG ceramic has over five times higher Nd<sup>3+</sup> ion doping level. Conventional ceramic laser has highly scattering loss which prevent the highly efficient laser oscillation. We are estimating an internal loss of laser cavity from the slope efficiency.

In summary, we developed highly Nd-doped YAG in ceramic for high power microchip laser. Four times higher laser output power in YAG ceramic compared

with conventional YAG single crystal was demonstrated.

### References

- 1) R. A. Fields *et al.*, *Appl. Phys. Lett.* **51**, 1885 (1987).
- 2) T. Taira *et al.*, *Opt. Lett.* **16**, 1955 (1991).
- 3) W. L. Nighan *et al.*, *Conf. Lasers and Electro-Optics*, OSA Tech. Dig.; Washington DC., paper CMD5 (1995).
- 4) M. D. Selker *et al.*, *Conf. Lasers and Electro-Optics*, OSA Tech. Dig.; Washington DC., paper CPD21 (1996).
- 5) T. Taira *et al.*, *TOPS* **19**, 430 (1998).

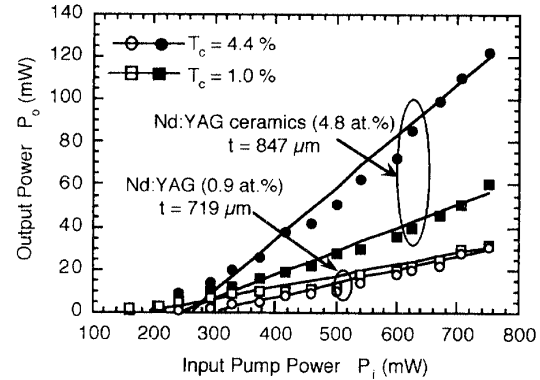


Figure 1. Input-output power characteristics of a diode-pumped Nd:YAG ceramic laser.

### VIII-D-4 Nondestructive Characterization of Quasi-Phase-Matched Wavelength Converter

KURIMURA, Sunao; UESU, Yoshiaki<sup>1</sup>  
(<sup>1</sup>Waseda Univ.)

We devised an observation technique of 180° domains in ferroelectric crystals by using Second Harmonic Generation (SHG) Microscope. The phase reversal of the SH wave accompanying inversion of spontaneous polarization is exploited to visualize domains. Interference between SH waves converts the phase information to the SH contrast. Domain mapping is achieved in LiNbO<sub>3</sub> and LiTaO<sub>3</sub> with nonlinear coefficients  $d_{33}$  and  $d_{22}$  under the microscope, which enables characterization of a periodically-poled structure in quasi-phase-matched wavelength converters in a nondestructive way. The validity of the technique is proved by another characterizing tool of destructive etching.

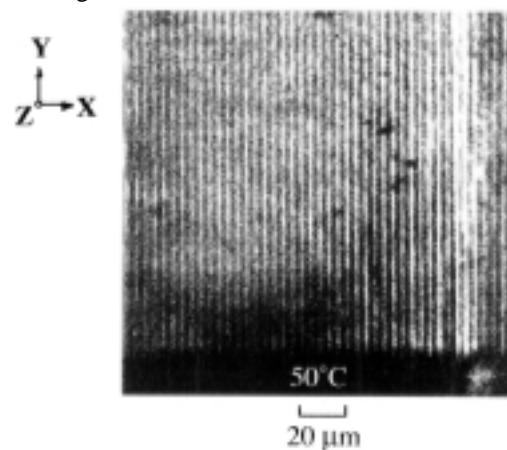


Figure 1. Photo of a Z-cut QPMLT device.